Colloids and Surfaces A: Physicochemical and Engineering Aspects 721 (2025) 137199

Contents lists available at ScienceDirect

Colloids and Surfaces A: Physicochemical and Engineering Aspects

journal homepage: www.elsevier.com/locate/colsurfa

Preparation and evaluation of mixed alginate-cyclodextrin hydrogels: From physicochemical, thermotropic to swelling characterization

Vasiliki Karali [a,1], Paraskevi-Evelina Goula [a,1], Georgia Patroklou [a], Elmina-Marina Saitani [a], George E. Baltatzis [b], Maria-Anna Gatou [c], Lykourgos C. Kontaxis [d], Evangelia A. Pavlatou [c], Stefanos P. Zaoutsos [d], Ioannis Trougakos [e], Georgia Valsami [a], Natassa Pippa [a,*], Stergios Pispas [f]

[a] Section of Pharmaceutical Technology, Department of Pharmacy, School of Health Sciences, National and Kapodistrian University of Athens, Panepistimioupolis Zografou, Athens 15771, Greece
[b] Imaging Core Facility, National and Kapodistrian University of Athens, Panepistimioupolis Zografou, Athens 15771, Greece
[c] Laboratory of General Chemistry, School of Chemical Engineering, National Technical University of Athens, Zografou Campus, Athens 15772, Greece
[d] LAMCO Laboratory, Department of Energy Systems, University of Thessaly, Gaiopolis Campus, Larisa 41500, Greece
[e] Department of Cell Biology and Biophysics, Faculty of Biology, National and Kapodistrian University of Athens, Panepistimioupolis Zografou, Athens 15771, Greece
[f] Theoretical and Physical Chemistry Institute, National Hellenic Research Foundation, 48 Vassileos Constantinou Avenue, Athens 11635, Greece

GRAPHICAL ABSTRACT

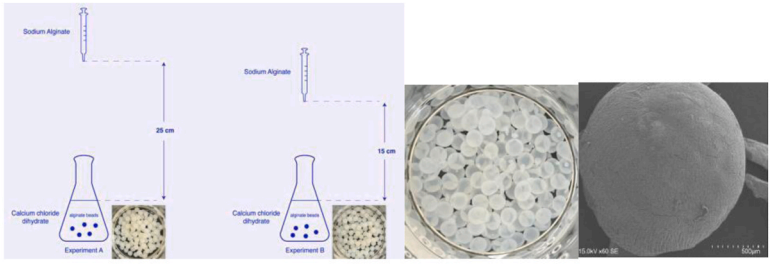

the impact of CDs' coexistence on the pH-responsiveness of alginate-based hydrogels

ARTICLE INFO

Keywords:
Hydrogels
Swelling
PH-responsiveness
Alginate
Cyclodextrins

ABSTRACT

The aim of this study is to develop hydrogel beads with the addition of cyclodextrins into a sodium alginate matrix and examine their swelling properties in different pH conditions. To achieve this, Methyl-β-Cyclodextrin (M-β-CD) and Hydroxypropyl-β-Cyclodextrin (HP-β-CD) were mixed with sodium alginate solution to form hydrogel beads. The formation of these beads was achieved at two different dropping distances (15 cm and 25 cm), and their swelling behavior was evaluated in two pH environments: SGF (simulated gastric fluid, pH 1.2) and SIF (simulated intestinal fluid, pH 6.8). The thermotropic behavior of the prepared alginate-based beads was analyzed using Differential Scanning Calorimetry (DSC) and Thermogravimetric Analysis (TGA). Scanning Electron Microscopy (SEM) was employed to evaluate the impact of the preparation method and the presence of

* Corresponding author.
E-mail addresses: natpippa@pharm.uoa.gr (N. Pippa), pispas@eie.gr (S. Pispas).
[1] Equal contribution to this work

https://doi.org/10.1016/j.colsurfa.2025.137199
Received 21 March 2025; Received in revised form 8 May 2025; Accepted 13 May 2025
Available online 14 May 2025

different types of cyclodextrins (CDs) on the beads' morphological characteristics. Results indicated that the addition of CDs had a substantial impact on the beads' swelling behavior and morphology, with HP-β-CD beads demonstrating the highest disintegration rate in SIF, mostly due to greater hydrophilicity and matrix interactions. The beads with CDs that were prepared at higher dropping distance exhibited increased porosity, enhancing water absorption. This study highlights the impact of CDs' coexistence on the pH-responsiveness of alginate-based hydrogels, underscoring their potential as delivery platforms for controlled drug release systems.

1. Introduction

The advancement of biomaterials has prompted research into alternative biocompatible materials, with alginate emerging as a focal point due to its promising properties. Alginate is an abundant natural polysaccharide obtained primarily from brown marine algae (class of Phaeophyceae) and certain bacteria, known for its unique gel-forming properties. It consists of alternating blocks of β-D-mannuronic acid and α-L-guluronic acid [1]. Alginate is highly suitable for a wide range of biomedical and clinical applications. Its non-toxic, biocompatible, cytocompatible, and biodegradable nature [2] allows it to be used in tissue engineering, aiming to provide mechanical integrity while transmitting mechanical signals to the cells [3]. It is also widely used in wound healing as well as in controlled drug release in the form of nanoparticles or microspheres, offering control of drug release rate and also delivery of the drug to a specific treatment target [4]. In recent years, as a deeper comprehension of the molecular structure and properties of alginate has been achieved, a variety of physicochemical cross-linking techniques has resulted in the development of distinct alginate hydrogel properties for a wide range of applications [5].

Moreover, a hydrogel is a cross-linked polymeric network that exhibits the ability to swell and retain a significant fraction of water within its structure, but it does not dissolve in water. The ability to swell emerges from hydrophilic functional groups attached to the polymeric backbone, while their resistance to dissolution arises from cross-links between network chains [6,7]. Hydrogels have been used as drug delivery systems, in wound dressings, tissue engineering and as temporary scaffolds for cells, since they offer the ability of controlled release of the encapsulated bioactive compounds. Additionally, they have several advantages such as physicochemical stability, biocompatibility and potential for oral administration [8,9].

The use of composite and functionalized materials using biodegradable polymers, ligand-based materials, and nanomaterials is of paramount importance for several applications, i.e., heavy metal ion removal, sensing, and environmental water purification. Several physicochemical and morphological techniques were developed for the evaluation of these functionalized hybrid materials [10–18]. Additionally, sustainable materials are usually hybrid formulations, i.e., chitosan-grafted nanocomposites, biodegradable carbohydrate-based polymeric materials, and organic-inorganic functionalized materials. Great emphasis is given during the preparation process of them to the surface interactions and interactions between the different materials [19–27].

Regarding cyclodextrins (CDs) (cyclomalto-oligo-saccharides), they comprise a family of biocompatible cage materials which have been developed during the last thirty years to improve the solubility, stability and the bioavailability of drugs [28]. CDs are a class of cyclic glucopyranose oligomers, obtained from starch by enzymatic action, that contain at least six d–(+)–glucopyranose units linked by α–(1, 4) glycosidic bonds, with a characteristic non-symmetrical toroidal shape that forms a truncated cone-shaped lipophilic cavity. The main native CDs are named α, β, and γ which comprise six, seven, and eight glucopyranose units, respectively. CDs have the capability to enclose compounds whose size and polarity are compatible with those of their cavity. This is attributed to their unique structure featuring a hydrophobic interior and a hydrophilic exterior. Due to their encapsulation capacity and their properties as complexing agents and carriers of different substances, they find wide utilization for fundamental and technology applications in the medical and pharmaceutical industry. CDs are promising compounds for solving major bioavailability problems such as inadequate solubility, poor dissolution rate, and limited stability of some agents, as well as increasing their effectiveness and decreasing unwanted side effects [29,30].

Considering all the above, CDs were chosen to be incorporated into alginate beads in a non-covalent, co-assembly based approach in contrast to previous reports where CDs were covalently connected to alginate. Namely, the CDs are expected to alter the physicochemical properties of the alginate beads due to their amphiphilic nature of encompassing hydrophobic/hydrophilic parts [31,32]. In parallel, in drug design and development, CDs are widely used for the improvement of encapsulation and loading efficiencies, as well as the bioavailability of APIs, especially those of low solubility. Furthermore, they exhibit controlled release properties, especially when they are used with other (bio-)functional excipients (i.e., block polymers, etc.). Last but not least, they can protect the sensitive APIs from degradation and enzymatic attack and improve their mucoadhesion properties [31,32]. Overall, it is interesting to study whether a simple co-assembly process involving alginate and CDs would meet these properties satisfactorily.

The grafting of β-CD to alginate via chemical synthesis was found to be effective for increased encapsulation efficiency and prolonged release of the model molecule methyl orange. The same CD was used for the increase of the solubility of edaravone, and the inclusion systems were encapsulated into sodium alginate and chitosan-based nanocomposites for achieving pH-controlled release [33]. The stoichiometry of the inclusion system was found to be important for controlling the release process [33]. Omtvedt et al. [34,35] designed and developed alginate hydrogel formulations functionalized with β-CD for the encapsulation and the local delivery of the anticancer API paclitaxel. The added value of this formulation was the reduction of the crystallization of the paclitaxel and its more effective diffusion and release from the hydrogel network [34,35].

β-CD is characterized by an ideal size of its cavity for the incorporation of molecular agents, a cost-effective production and the ability to ameliorate the bioavailability and the toxicological profile of active pharmaceutical ingredients. Such characteristics are making β-CD a highly valuable material for biomedical applications. However, its low aqueous solubility remains a significant challenge [36,37]. To overcome this limitation, derivatives of β-CD have been developed by the substitution of its hydroxy groups. In our experiment, we mixed Methyl-β-CD (M-β-CD) or/and hydroxypropyl-β-cyclodextrin (HP-β-CD) with sodium alginate to create beads, allowing us to observe not only their morphology but also their swelling ability, in comparison to sodium alginate beads without the addition of CDs.

The rationale for using M-β-CD and HP-β-CD stems from their specific physicochemical properties that make them more suitable for our studies, especially their ability to increase solubility, to form more stable and efficient complexes and induce low cytotoxicity [38].

The aim of this study is to prepare hydrogel beads consisting of sodium alginate, with and without CD additives, to examine their formation at varying dropping distances from a calcium chloride solution (15 and 25 cm) and investigate their swelling behavior in two different dispersion media: simulated gastric fluid (SGF, pH 1.2) and simulated intestinal fluid (SIF, pH 6.8). The simulation of the stomach and intestinal conditions is important when studying the swelling behavior of the

beads, since such environments are linked to their performance, particularly for drug delivery systems. In acidic gastric conditions, the beads should prevent early release owing to low pH, whereas in intestinal pH conditions, they should disintegrate and release their contents. For example, a study on pectin-chitosan hydrogel beads shows that they do not degrade in the stomach whereas they release their content in the intestines. This differentiation makes them ideal candidates for targeted delivery [39].

This study shows how the presence of CDs affects the pH sensitivity of alginate-based hydrogels, emphasizing their promise for use in controlled drug delivery systems. This hybrid system exhibits unique properties coming from the blending of different materials, combining the advantages of each material, i.e., the pH responsiveness of alginate and the compartmentalized structure of CDs, with the ability to encapsulate both hydrophilic and lipophilic compounds. The innovation of the present work lies in the fact that for the first time in the literature, an empirical design parameter (the distance for the preparation of alginate beads, as visualized Scheme 1) has been investigated, to determine whether it is Critical Process Parameter (CPP) for the development of alginate beads with or without the presence of CD. Furthermore, a comparison study was performed of the morphological, thermotropic, swelling properties of alginate beads with the presence of different in nature CDs. In other words, this investigation aims to highlight the enhanced functional properties of hybrid alginate-based hydrogels using various physicochemical, morphological, and thermotropic techniques to advance the design and development of materials for several applications in drug delivery, targeting, and pharmaceutical technology.

2. Materials and methods

2.1. Materials

Low viscosity alginic acid sodium salt, calcium chloride dihydrate ($CaCl_2$•2 H_2O) and the derivatives of β-CD, M-β-CD and HP-β-CD, were purchased from Sigma-Aldrich Chemical Co (St. Louis, MO, USA). Deionized water was used as the solvent. Simulated gastric fluid (SGF, pH 1.2) and simulated intestinal fluid (SIF, pH 6.8) were prepared as described in United States Pharmacopeia (USP) guidelines. No hazardous components existed in the method of the preparation, since all the materials used are biocompatible (see in the Introduction) and of analytical grade. The solvent that we used was deionized water, and the biorelevant media were prepared under the guidelines of USP.

2.2. Methods

2.2.1. Preparation of sodium alginate beads

Sodium alginate (SA) beads were prepared following a protocol described in the literature, with some modifications [40]. A SA solution was prepared in ultrapure water at a concentration of 4 % w/v, with magnetic stirring under heating to achieve alginate's faster and complete dissolution for 10–15 minutes. A solution of $CaCl_2$•$2H_2O$ was then prepared at a concentration of 0.1 M. While the literature's protocol used a dropping distance of 6 cm, here in our protocol we used two different dropping distances, 15 cm and 25 cm (Scheme 1). This was done with the aim of investigating the effect of the dropping distance on the shape, size, and morphology of the beads [40]. The SA solution was placed in a syringe on a support stand positioned firstly 25 cm above the surface of the $CaCl_2$•$2H_2O$ solution (experiment A) and afterwards 15 cm above the surface (experiment B), and the drop flow of the solution from the syringe was initiated, leading to bead formation. The duration required for the consumption of the SA solution was 1 minute and 30 seconds in experiment A and 1 minute and 40 seconds in experiment B. The beads were then rinsed with deionized water and placed on a petri dish, after previously being separated from each other. The petri dishes (A) and (B) were finally placed in a drying oven at 33°C. The beads after the crosslinking process/formation are visualized in Fig. 1.

2.2.2. Preparation of sodium alginate beads with cyclodextrins

First, a M-β-CD solution in water was prepared with a concentration of 10 mg/ml, followed by magnetic stirring under heating for 5 minutes. Similarly, an aqueous solution of HP-β-CD was prepared at the same

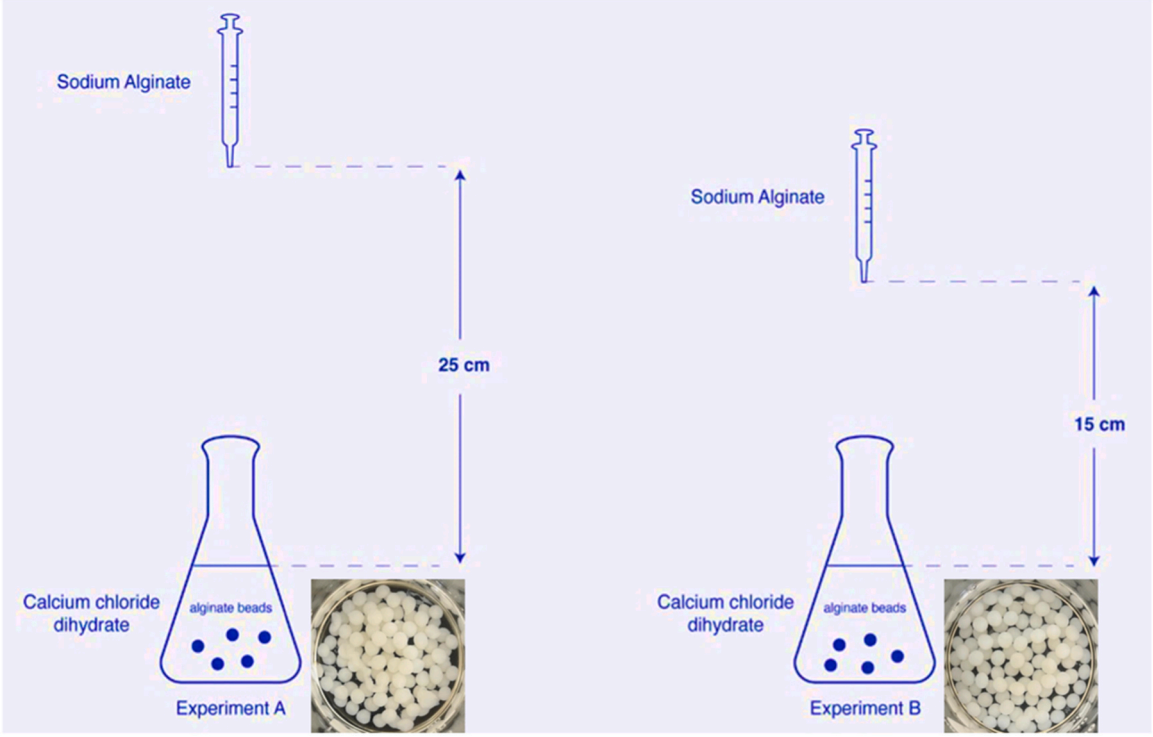

Scheme 1. The preparation protocols.

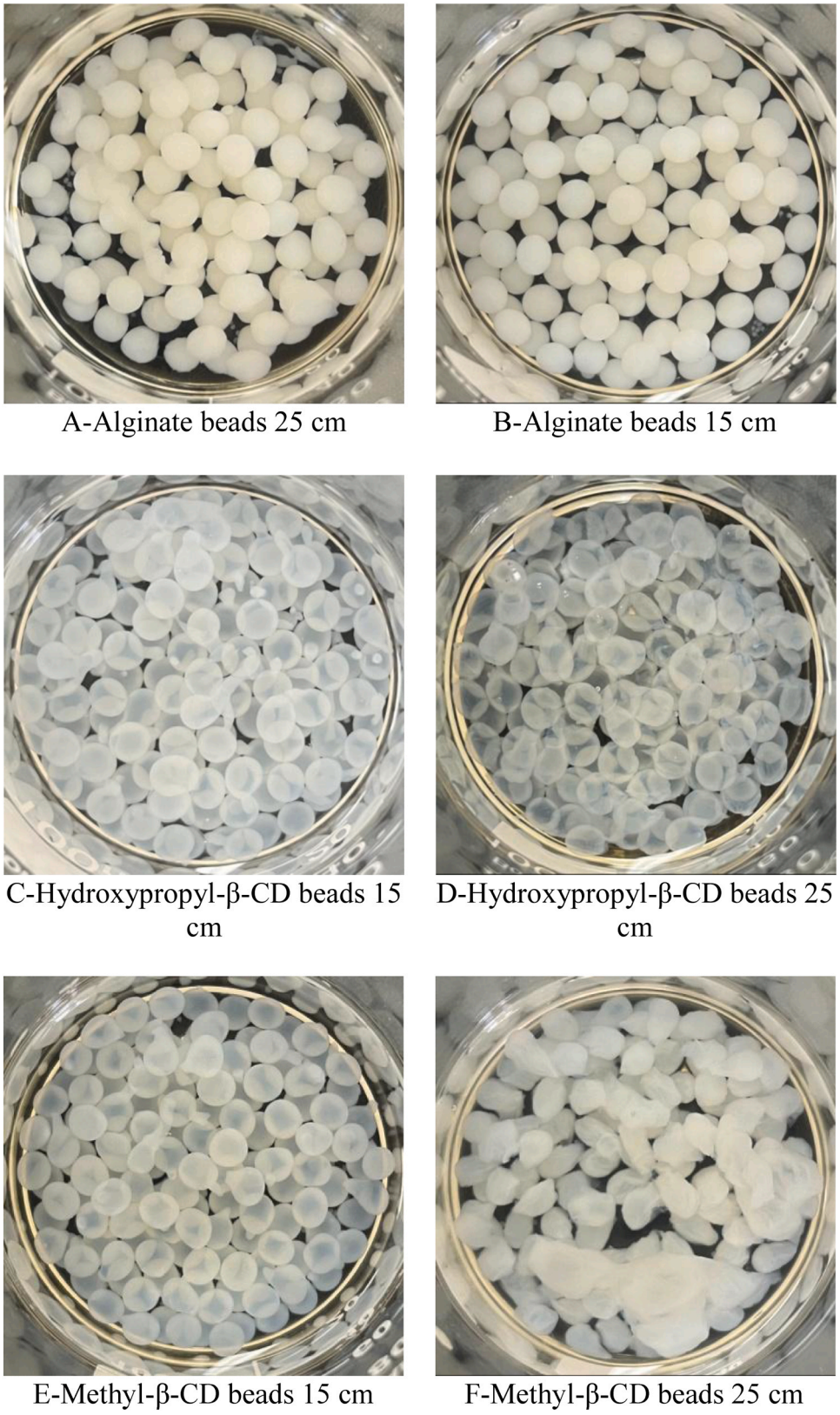

Fig. 1. Images captured after beads' formation, released from a syringe at two different dropping heights (15 cm and 25 cm). Beads consist of SA, M-β-CD or HP-β-CD.

concentration, with magnetic stirring under heating for 5 minutes. Afterwards, a 4 % w/v SA solution in water was prepared, with magnetic stirring under heating for approximately 15 minutes to ensure complete dissolution. Once the SA solution was ready, 10 ml of the solution were transferred into a beaker. This process was repeated three more times leading to four separate beakers of 10 ml each. To two of the beakers, 1 ml of the M-β-CD solution was added, while 1 ml of the HP-β-CD solution was added to the other two beakers. Subsequently, one of the solutions containing M-β-CD was placed in a syringe on a support stand above the surface of the $CaCl_2$•2 H_2O solution, at a distance of 25 cm. The drop flow of the solution from the syringe was initiated, and the bead formation was observed. The time required for the complete consumption of the solution was recorded as 58 seconds. After the formation of beads, they were rinsed with deionized water and carefully separated before being placed on a petri dish. The same procedure was repeated with a solution containing SA and 1 ml of HP-β-CD. This solution was also placed in the syringe and allowed to drop into the calcium chloride solution. The time needed for the solution to be fully consumed in this case was recorded as 1 minute. All the steps which had taken place in 25 cm were repeated, but this time by adjusting the distance between the tip of the syringe and the surface of the calcium chloride solution to 15 cm. For the SA solution containing M-β-CD, the solution's consumption took 1 minute and 4 seconds, while for the SA solution containing HP-β-CD, it took 1 minute and 15 seconds. Finally, all four petri dishes containing the beads were placed in a drying oven at 33°C. Table 1 presents the composition of all prepared formulations. Six different formulations were developed using two dropping distances: 15 cm and 25 cm. Formulations A, C, and F correspond to SA, SA:HP-β-CD, and SA:M-β-CD, respectively. The formulations prepared with a 25 cm dropping distance are referred to as B, D, and F.

2.2.3. Swelling studies

Swelling studies of all prepared formulations were conducted under two different pH conditions: 1.2 and 6.8. The beads used in this experiment, the ones produced previously, are categorized as follows: A:Sodium Alginate (25 cm), B:Sodium Alginate (15 cm), C:HP-β-CD (15 cm), D: HP-β-CD (25 cm), E: M-β-CD (15 cm), and F: M-β-CD (25 cm) (Table 1). At the beginning of the experiment, the weight of five beads from each petri dish was measured. A solution with a pH value equal to 1.2 was added to six separate beakers and half of the beads from each petri dish were then placed into each beaker. At 15-minute intervals, five beads were removed from each beaker, weighed, and then returned to their corresponding beakers. This process was repeated every 15 minutes for a total duration of one hour. The one-hour duration of the experiment was sufficient as the beads tend to swell less and dissolve slowly in acidic pH. This behavior can be attributed to the protonation of alginate's carboxyl groups at low pH values, reducing their interaction with water molecules and conclusively the system required less time for measurable changes to occur (minimal swelling and release) [41].

After 60 minutes, the solutions were discarded from each beaker, while keeping the beads inside them. A new solution with a pH value adjusted to 6.8 was added to each beaker and the previously described procedure was repeated. Beads were removed, weighed, and returned to their corresponding beakers every 15 minutes. However, this phase of the experiment lasted 1 hour and 35 minutes, as the expected greater swelling and faster dissolution at pH 6.8 required more time to complete this process [41].

The dynamic weight change of the beads over time was calculated according to Eq. (1) and is called swelling ratio Qs:

$$Qs(\%weight\ change) = \frac{W_t - W_i}{W_i} \times 100 \quad (1)$$

where W_t is the weight of the beads in the swollen state and W_i is the initial weight of the beads [42].

2.2.4. Thermogravimetric analysis (TGA)

Thermogravimetric analysis was performed utilizing a Mettler Toledo TGA/DSC 1 HT apparatus (Mettler Toledo GmbH, Greifensee, Switzerland). Measurements were conducted under air atmosphere in the range 30–900 °C and a heating rate equal to 10 °C/min.

2.2.5. Differential scanning calorimetry (DSC)

Thermal characterization of the specimens was conducted by means of DSC measurements, via a TA Q200 (New 200 Castle, DE, USA). The DSC device was operated in the temperature range of 30–300 °C at a 10 °Cmin^{-1} ramp in endothermic mode. DSC experiments were conducted under a steady flow of nitrogen. Each sample was analyzed by placing 1.5–3.0 mg samples sealed in aluminum pans. An empty aluminum pan was used as a reference during the analyses. The data obtained from the DSC measurements (enthalpy changes ΔH, characteristic transition and Peak Temperature) were analyzed using TA Universal Analysis software.

2.2.6. Scanning electron microscopy (SEM)

Samples were fixed on stubs with carbon tape and coated with gold for 30 sec in a Leica EM ACE200 Coating System (Leica Microsystems CMS GmbH, DE). Subsequently samples were viewed and photographed in a Hitachi SU3800 Scanning Electron Microscope at various magnifications at 15 kV. (Hitachi, High Tech Corporation, JP).

Table 1
Composition of all prepared formulations, dropping distance between the syringe tip and the surface of the CaCl2•2H_2O solution, total dispensing time for the preparation of each formulation, beads size after preparation and drying.

Formulation		Dropping distance (cm)	Total dispensing time (seconds)	Size of the beads after the preparation process	Size of dried beads (SEM images)
A	SA	25	90	≈ 3.2 mm	750μm
B	SA	15	120	≈ 3.5 mm	900μm
C	SA:HP-β-CD	15	75	≈ 3.6 mm	800μm
D	SA:HP-β-CD	25	60	≈ 4.0 mm (agglomerates)	1100μm
E	SA:M-β-CD	15	64	≈ 3.4 mm	1000μm
Z	SA:M-β-CD	25	58	≈ 3.8 mm (agglomerates)	1150μm

3. Results and discussion

The physicochemical evaluation and characterization of functionalized and composite materials are useful for the identification of their morphology, surface, and microstructural features using imaging techniques, i.e., SEM. Additionally, thermal stability and the durability of the hybrid materials in real, moisture content and/or accelerating aging conditions should be analyzed in order to evaluate the degradation process utilizing the TGA technique [43–46].

3.1. Thermal behavior of mixed sodium alginate beads

Firstly, we used TGA in order to study the thermal stability of the alginate beads with or without the presence of CDs, as well as with the different preparation protocols. For all the samples, the initial water loss is observed below 200°C (Fig. 2). It seems that the preparation protocol and/or the presence of CDs do not play a significant role in the evaporation of the water molecules from the alginate beads. According to the literature, weight loss during this step can be associated with the oxidation process of sugars (guluronic and mannuronic) in alginate biopolymer chains, which relates to the small exothermic peaks in the DSC curves [47]. The main decomposition step is observed between 250 and 400°C. For this decomposition step, it seems that the distance of

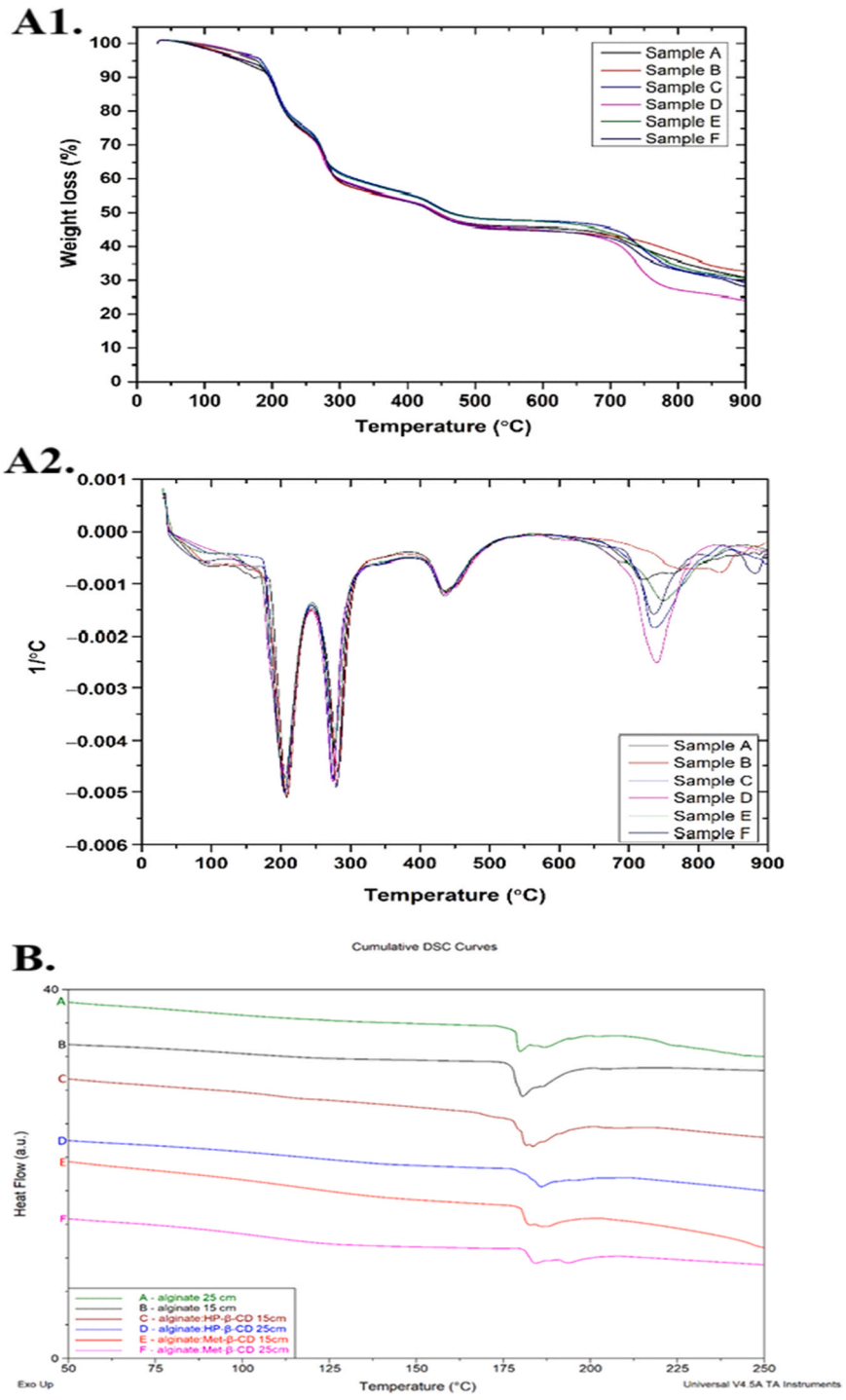

Fig. 2. A1. TGA, A2. TGA derivatives and B. DSC curves of all the prepared alginate beads with or without the presence of CDs.

15 cm is crucial for weight loss since both CDs have identical thermal stability behavior. In other words, the preparation at 15 cm dropping distance is responsible for lower weight loss in the case of samples C and E. All the other samples exhibited similar behavior. The last observation means that the breaking down of glycosidic bonds between the guluronic and mannuronic acids of alginate biopolymer was not affected by the presence of CDs. Above 700°C, each sample exhibited different behavior regarding the amount of weight loss. We should point out that the pure alginate beads showed a lower weight loss in comparison to the mixed alginate: CD beads (Fig. 2). The highest weight loss was observed for sample D. To conclude, the presence of the CDs derivatives can ameliorate the thermal stability of the alginate beads when the mixed beads are prepared at lower dropping distances.

We also used DSC in order to investigate the thermal behavior of sodium alginate beads in the presence of CDs (Fig. 3). The role of the distance between the alginate dispersion and the calcium solution for the cross-linking process is also examined. According to the literature, the pure alginate biopolymer exhibits a broad endothermic peak that begins around 145°C, while the sodium alginate exhibits an endothermic transition peak at 190°C and the gelation of the alginate with calcium cations is ten degrees lower in comparison to sodium alginate [48–50]. The same broad transition peak around 180°C was observed for

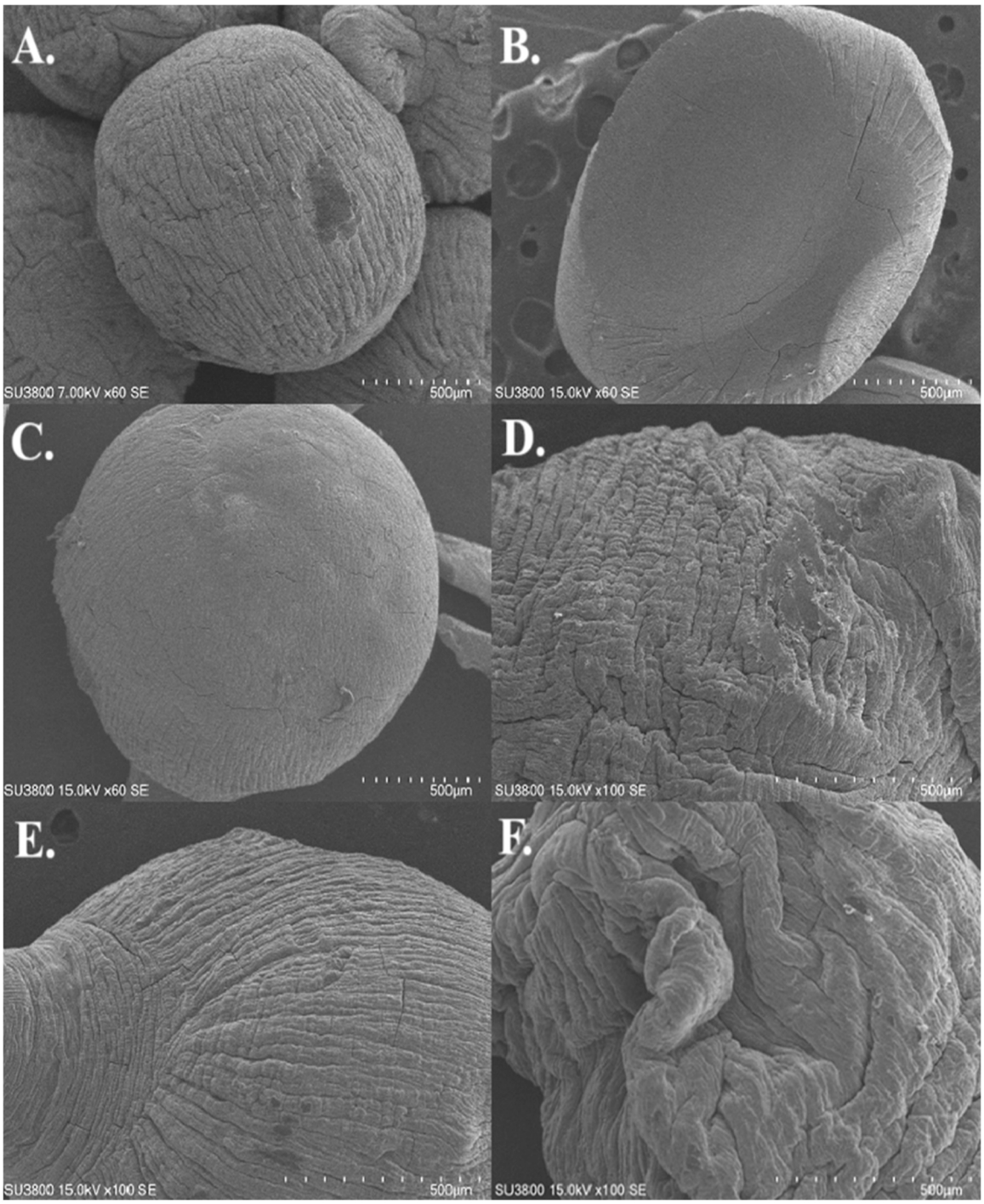

Fig. 3. SEM images of A-alginate 25 cm, B- alginate 15 cm, C- alginate:HP-β-CD 15 cm, D- alginate:HP-β-CD 25 cm, E- alginate:M-β-CD 15 cm and F- alginate:M-β-CD 15 cm (scale bar at 500μm).

sample A, which is sodium alginate crosslinked beads prepared at 25 cm. It seems that the preparation protocol affects the transition peak for samples A and B to some extent. On the other hand, the enthalpy of transition increases, meaning that more energy is required for sample B, which was crosslinked with shorter dropping distances in comparison to sample A (Fig. 3). In our opinion, the endothermic peaks are quite different due to the different percentage loss of water associated with the hydrophilic groups of sodium alginate [48–50]. It should be noted that the DSC study of the pure CDs was evaluated in our previous publication [51]. The HP-β-CD exhibits an endothermic sharp peak at 147°C, while the M-β-CD has a broad endothermic peak at 180°C. The difference in the surface of these CDs is strongly associated with the different water loss structure at the hydrophilic outer surfaces. The presence of CDs leads to a higher transition temperature for all the samples. For the HP-β-CD, the increase of the peak temperature is higher for both preparation protocols in comparison to M-β-CD. Generally, the addition of other excipients of active substances causes an increase in the temperature of the transition peak of sodium alginate. The preparation protocol also affects the ΔH values (Table 2).

For the shorter distance, the ΔH values are increased for both the mixed sodium alginate beads. This behavior of the mixed systems is the opposite in comparison to the pure sodium alginate beads (Table 2,

Table 2
Calorimetric heating profiles of the prepared alginate beads with or without the presence of CDs.

Specimen	Enthalpy Change ΔH (J/g)	Peak temperature (°C)
A-alginate 25 cm	183.8	179.8
B-alginate 15 cm	245.9	177.4
C-alginate:HP-β-CD 15 cm	282.8	183.5
D-alginate:HP-β-CD 25 cm	122.7	185.9
E-alginate:M-β-CD 15 cm	130.5	185.7
F-alginate:M-β-CD 15 cm	120.7	184.2

Fig. 2B). The presence of the CDs alters the hydrogen bonds and the van der Waals interactions between these materials. The van der Waals interactions due to the hydrophobic cavities and the hydrogen bonds due to the hydrophilic outer surfaces of CDs are changed during the crosslinking process, in which the distance from the calcium cations plays a key role. Overall, thermal analysis techniques are used to confirm how the mixture or blending process during the preparation protocol can alter the thermotropic behavior of biopolymers—in our case, the alginate—in the presence of other materials—in our case, the CDs. The thermal transition and its changes confirm the physicochemical interactions between the different materials in nature [52–56].

3.2. Morphological characterization of the beads

To investigate the factors affecting beads' morphology, SA beads were prepared by dropping a SA solution into a $CaCl_2 \bullet 2H_2O$ one from two heights (15 cm and 25 cm), with or without the addition of M-β-CD and HP-β-CD. The effect of dropping distance on beads' shape, size, and light permeability was assessed, alongside the impact of CD incorporation on beads' uniformity and transparency.

When it comes to examining the morphological characteristics of the beads, it is evident that the beads containing pure alginate, have round, completely spherical and homogeneous shape and that they enable light scattering (Fig. 3). These observations align with alginate's inherent ability to form beads through ionotropic gelation in the presence of calcium ions, combined with the controlled experimental conditions that promote the formation of uniformly shaped beads.

The morphological characterization of M-β-CD and HP-β-CD beads shows clear differences in size, uniformity, shape, and light permeability, as depicted in Fig. 1. On the one hand, the HP-β-CD beads retain their relative size uniformity for both 15 cm and 25 cm addition protocols; on the other hand, M-β-CD ones experience such uniformity for the 15 cm samples but show size variation for the 25 cm case, where they also form agglomerates. In terms of shape, both the beads of M-β-CD and those of HP-β-CD are mainly spherical for the 15 cm case, with some teardrop formations, while for 25 cm, these beads become mainly irregular and take angular shapes. The irregular sizes of the beads at higher dropping distances between the two solutions can be due to the increased velocity which causes the droplets to hit the CaCl2•2H2O solution with more force leading to less uniform or slightly deformed beads. Light permeability varies as well, with M-β-CD beads indicating higher light scattering for 25 cm, something that can also be observed, though to a lesser extent, for the 15 cm case. In contrast, HP-β-CD beads at both dropping lengths exhibit increased light permeability. These morphological features bring out the diversity in structure between M-β-CD and HP-β-CD beads, which might be due to intrinsic material properties or environmental interactions. More specifically, the higher hydrophilicity of HP-β-CD and the occurrence of better intermolecular interactions with the alginate polymer chains through hydrogen bonding, due to the presence of hydroxypropyl groups, promotes better dispersion of HP-β-CD within the alginate matrix, forming a more cohesive and transparent bead structure that allows light to pass. On the other hand, the M-β-CD beads, which are notably less hydrophilic, may form small clusters within the bead matrix, leading to structural irregularities and thereby increasing light scattering.

The morphological characterization of the dried samples at the microscale was conducted by SEM. Fig. 3 and Fig. 4 show the surface morphology of the beads in different scales, at 500 μm and 20 μm, respectively. All the alginate beads with and without CDs are spherical. The preparation protocol for the formation of the beads affects the microstructure of the crosslinked alginate beads, as is shown in both scalebars (Figs. 3A, 3B, 4A, and 4B). The size of the dried beads formed at 15 cm dropping distance is smaller in comparison to those formed at 25 cm (Fig. 3A and B). The lower distance caused more compact surface morphology with a higher number of "valleys" and "rivers," as it is shown in Fig. 4B. Generally, the presence of other materials with -OH groups (i.e., glycerol) results in the presence of "craters" on the surface of the dried alginate beads [57]. The presence of the CDs alters the morphology and the size of the prepared dried beads. This observation is in line with the visual observation before the drying process, which is described above. The size of the samples with the M-β-CD is higher in comparison to pure and HP-β-CD (Fig. 3C, D, E, and Z). Namely, HP-β-CD is responsible for the cracks in the surface structure during the preparation of the beads at the distance of 15 cm. These cracks are not visible at the distance of 25 cm. The higher amount of water molecule absorption due to the higher hydrophilicity of the HP-β-CD is probably responsible for the formation of these cracks. These cracks are formed during the evaporation of water during the drying process. Furthermore, the "brain-like structure" is observed for the mixed alginate beads with M-β-CD. It seems that the different distances during the crosslinking process did not affect the morphological characteristics of the SA: M-β-CD beads. Probably, the more hydrophobic nature of M-β-CD is responsible for the limited absorption of water molecules and a more homogenous drying process, causing a smooth surface microstructure. To the best of the authors' knowledge, this is the first time SEM images are obtained for mixed alginate beads containing CDs.

3.3. Swelling studies

In SGF (pH 1.2), all dried beads exhibited slight swelling within the first hour, gaining weight due to the hydration of hydrophilic carboxylate groups. As shown in Fig. 5, at the same time point, formulation D (SA:HP-β-CD, dropping distance of 25 cm), showed the most increased swelling with a weight increase of approximately 300 %, whereas the SA beads, A and B, displayed the least swelling.

At higher pH values, the carboxyl groups of alginate become deprotonated, enhancing their ability to interact with water, leading to greater swelling and faster dissolution. In SIF (pH 6.8), beads containing β-CDs are expected to exhibit the highest swelling and disintegrate faster than the alginate beads (A and B) due to the presence of hydroxyl (–OH) groups in their structure, which contribute to their polarity and dissolution. In contrast, as supported by the literature [42], alginate-based beads are expected to swell less and disintegrate later than those containing β-CDs.

According to the diagram, SA beads without CDs exhibit small weight change throughout the duration of the experiment. This can be attributed to the structural and chemical properties of alginate. Specifically, its alternating blocks of β-D-mannuronic acid and α-L-guluronic acid form ionic bonds with calcium ions, creating a stable ionic network that can retain water while limiting the swelling capacity.

It is observed that both M-β-CD and HP-β-CD at the distance of 25 cm demonstrated a significant weight change. This phenomenon could be explained by several combined factors related to the beads' structure and formation dynamics [58]. When the solution is dropped from a greater height (25 cm), it hits the calcium chloride solution with more kinetic energy. This impact can cause rapid gelation, leading to a less compact cross-linked structure and greater porosity within the bead matrix. As a result, a looser network structure provides more space within the matrix, allowing more water to penetrate and increasing the beads' swelling capacity. Moreover, it cannot be overlooked that the higher drop height causes beads to form irregular and less spherical

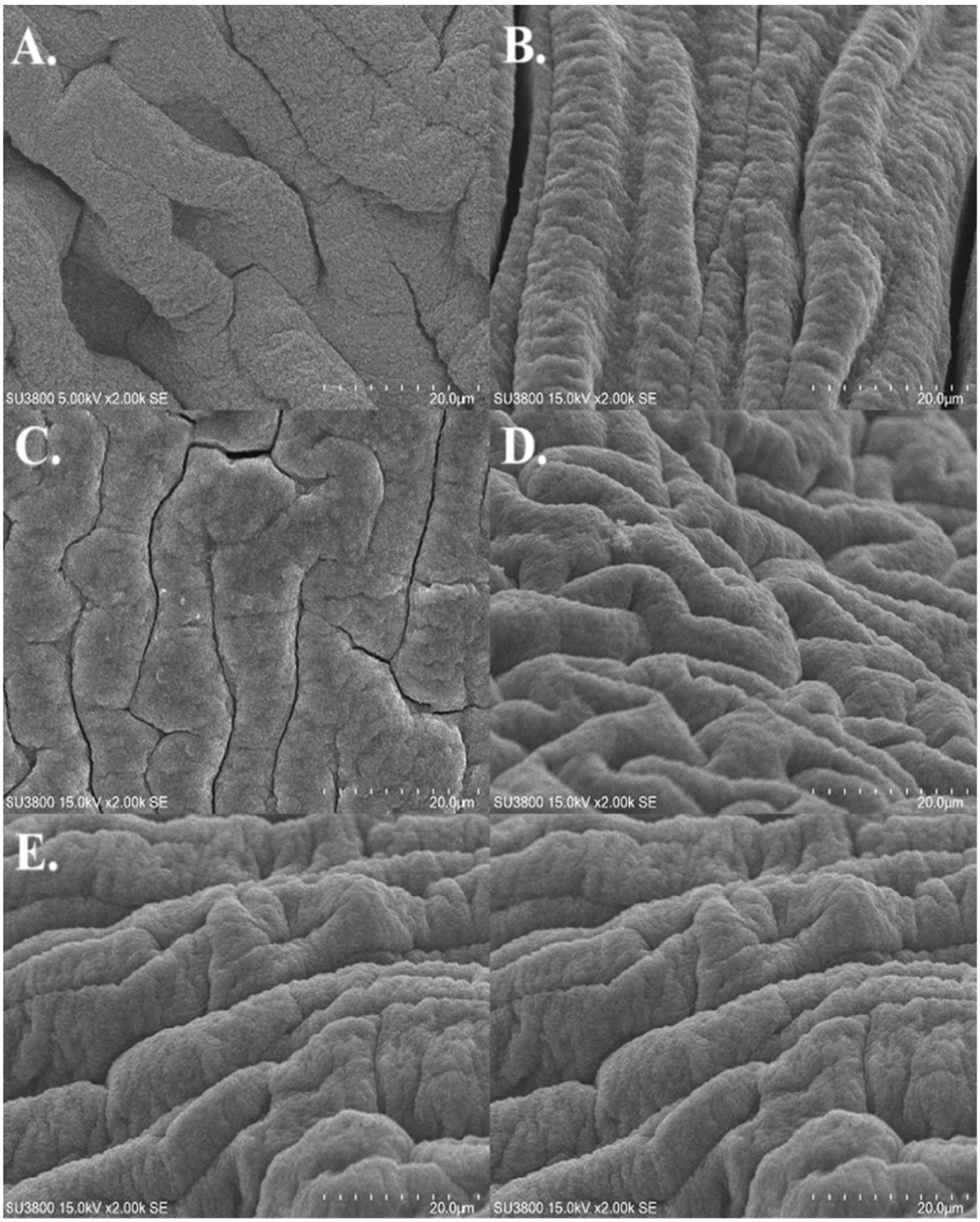

Fig. 4. SEM images of A-alginate 25 cm, B- alginate 15 cm, C- alginate:HP-β-CD 15 cm, D- alginate:HP-β-CD 25 cm, E- alginate:M-β-CD 15 cm and F- alginate:M-β-CD 15 cm (scale bar at 20μm).

shapes. These irregularities increase the surface area, which enhances water absorption, leading to a greater swelling ratio, especially in a suitable pH environment, such as the pH of 6.8. Finally, it is important to note the influence of CDs on network looseness. As explained before, both M-β-CD and HP-β-CD, affect the cross-linking density of the alginate matrix differently than alginate alone and those interactions create additional space or weak points within the matrix, making the structure more susceptible to swelling. At 25 cm drop, where the beads are already less tightly packed, the presence of CDs enhances this effect, allowing water to interact more with the matrix.

Another inference derived from the analysis and the delineation of beads' swelling behavior is that all the beads containing CDs, after reaching their maximum swelling ability, start to disintegrate, while the beads containing alginate do not show any signs of disintegration at the duration of our experiment. This fact is entirely reasonable and aligns with the above conclusions regarding the beneficial capacity of CDs in the dissolution of beads and the improvement of their swelling. It appears, HP-β-CD at 25 cm are the only beads that completely disintegrate at the end of the experiment, due to the combination of higher hydrophilicity of hydroxypropyl groups and the higher dropping distance.

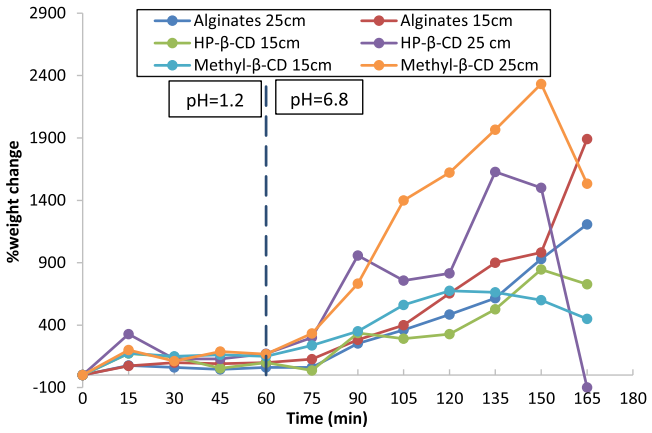

Fig. 5. Swelling profiles of SA beads (red: 15 cm dropping height, blue: 25 cm), SA:M-β-CD beads (light blue: 15 cm, orange: 25 cm), and SA:HP-β-CD beads (green: 15 cm, purple: 25 cm) over time in SGF (up to 60 min) and SIF (up to 135 min).

These mixed beads disintegrate faster in comparison to all other formulations.

Taking into account both the irregular shape of the HP-β-CD:alginate beads, as evidenced by the cracks on the surface of the dried formulation observed in the SEM images, and the presence of a larger network of hydrogen bonds (as discerned from the DSC curves), the fast disintegration of this system becomes more comprehensible. These cracks in the surface suggest a less cohesive and more fragile structure, which could facilitate a faster breakdown during the swelling studies in pH= 6.8. This combination of structural weaknesses and extensive hydrogen bonding explains to our opinion why the system dissolves much more rapidly compared to the other pure and mixed alginate beads, where the network may be more stable, or the surface integrity is more intact. Finally, the approach of this study is evidently sustainable, as it promotes efficiency and aligns principles of green engineering and sustainability [59].

4. Conclusions

This study examined the preparation and characterization of sodium alginate beads, with and without CD additives, and examining their swelling behavior under simulated gastric and intestinal conditions. The results demonstrated that the addition of β-CD derivatives (M-β-CD and HP-β-CD) significantly enhanced the swelling and disintegration properties of the alginate beads, in comparison to those without CDs. According to morphological evaluation, beads formed at greater distance (25 cm) exhibited uneven shapes, which were associated with a higher swelling capacity, likely due to a more porous structure that allows water penetration.

In simulated gastric fluid (SGF) where pH was equal to 1.2, the alginate beads displayed minimal swelling, confirming the alginate's predicted stability in acidic conditions. On the contrary, CD-containing beads demonstrated significant swelling and rapid disintegration in simulated intestinal fluid (SIF) where pH was 6.8, indicating their potential use for targeted drug delivery applications. Noticeably, because of its hydrophilic properties and the dynamic interactions within the alginate matrix, HP-β-CD exhibited the highest disintegration rate.

In conclusion, after considering the findings, it may be inferred that CDs have a promising contribution to enhancing the performance of alginate-based hydrogels for biomedical applications, especially in controlled drug release systems. Future research should further investigate the mechanisms behind the interactions between alginates and CDs, potentially leading to optimized formulations for more effective and targeted therapies.

Funding sources

This research received no external funding.

CRediT authorship contribution statement

Trougakos Ioannis: Supervision, Formal analysis. **Pavlatou Evangelia A.:** Supervision, Formal analysis. **Zaoutsos Stefanos P.:** Supervision, Formal analysis. **Gatou Maria-Anna:** Methodology, Formal analysis. **Kontaxis Lykourgos C.:** Methodology, Formal analysis. **Saitani Elmina-Marina:** Writing – original draft, Methodology, Formal analysis. **Baltatzis George E.:** Methodology, Formal analysis, Data curation. **Goula Paraskevi-Evelina:** Formal analysis, Data curation. **Pispas Stergios:** Writing – review & editing, Supervision. **Patroklou Georgia:** Formal analysis, Data curation. **Valsami Georgia:** Supervision, Methodology. **Karali Vasiliki:** Formal analysis, Data curation. **Pippa Natassa:** Writing – review & editing, Writing – original draft, Supervision, Methodology, Investigation, Conceptualization.

Declaration of Competing Interest

The authors declare that they have no known competing financial interests or personal relationships that could have appeared to influence the work reported in this paper.

Acknowledgments

None.

Data availability

The data in this manuscript are not confidential.

References

[1] J. Sun, H. Tan, Alginate-based biomaterials for regenerative medicine applications, Materials 6 (4) (2013) 1285–1309, https://doi.org/10.3390/ma6041285.
[2] M.Z.I. Mollah, H.M. Zahid, Z. Mahal, M.R.I. Faruque, M.U. Khandaker, The usages and potential uses of alginate for healthcare applications, Front. Mol. Biosci. 8 (2021), https://doi.org/10.3389/fmolb.2021.719972.
[3] J.L. Drury, R.G. Dennis, D.J. Mooney, The tensile properties of alginate hydrogels, Biomaterials 25 (16) (2004) 3187–3199, https://doi.org/10.1016/j.biomaterials.2003.10.002.
[4] N.T.T. Uyen, Z.A.A. Hamid, N.X.T. Tram, N. Ahmad, Fabrication of alginate microspheres for drug delivery: a review, Int. J. Biol. Macromol. 153 (2020) 1035–1046, https://doi.org/10.1016/j.ijbiomac.2019.10.233.
[5] Y. Ren, Q. Wang, W. Xu, M. Yang, W. Guo, S. He, W. Liu, Alginate-based hydrogels mediated biomedical applications: a review, Int. J. Biol. Macromol. 279 (2024) 135019, https://doi.org/10.1016/j.ijbiomac.2024.135019.
[6] E.M. Ahmed, Hydrogel: Preparation, characterization, and applications: a review, J. Adv. Res. 6 (2) (2015) 105–121, https://doi.org/10.1016/j.jare.2013.07.006.
[7] Y. Li, G. Huang, X. Zhang, B. Li, Y. Chen, T. Lu, T.J. Lu, F. Xu, Magnetic hydrogels and their potential biomedical applications, Adv. Funct. Mater. 23 (6) (2013) 660–672, https://doi.org/10.1002/adfm.201201708.
[8] S.R. Van Tomme, G. Storm, W.E. Hennink, In situ gelling hydrogels for pharmaceutical and biomedical applications, Int. J. Pharm. 355 (1) (2008) 1–18, https://doi.org/10.1016/j.ijpharm.2008.01.057.
[9] N. Pippa, T. Sentoukas, S. Pispas, C. Demetzos, A. Papalois, N. Bouropoulos, pH-responsive polymeric nanoassemblies encapsulated into alginate beads: morphological characterization and swelling studies, J. Polym. Res. 25 (5) (2018) 117, https://doi.org/10.1007/s10965-018-1519-1.
[10] M.S. Hossain, M.A. Shenashen, M.E. Awual, A.I. Rehan, A.I. Rasee, R.M. Waliullah, K.T. Kubra, M.S. Salman, M.C. Sheikh, M.N. Hasan, et al., Benign separation, adsorption, and recovery of rare-earth Yb(III) ions with specific ligand-based composite adsorbent, Process Saf. Environ. Prot. 185 (2024) 367–374, https://doi.org/10.1016/j.psep.2024.03.026.
[11] M.S. Salman, H. Znad, M.N. Hasan, M.M. Hasan, Optimization of innovative composite sensor for Pb(II) detection and capturing from water samples, Microchem. J. 160 (2021) 105765, https://doi.org/10.1016/j.microc.2020.105765.
[12] M.E. Awual, M.S. Salman, M.M. Hasan, M.N. Hasan, K.T. Kubra, M.C. Sheikh, A. I. Rasee, A.I. Rehan, R.M. Waliullah, M.S. Hossain, et al., Ligand imprinted composite adsorbent for effective Ni(II) ion monitoring and removal from contaminated water, J. Ind. Eng. Chem. 131 (2024) 585–592, https://doi.org/10.1016/j.jiec.2023.10.062.

[13] M.N. Hasan, M.S. Salman, A. Islam, H. Znad, M.M. Hasan, Sustainable composite sensor material for optical cadmium(II) monitoring and capturing from wastewater, Microchem. J. 161 (2021) 105800, https://doi.org/10.1016/j.microc.2020.105800.
[14] K. Li, S.T. Matkarimov, W. Xiao, C. Liu, S. Yang, Fundamental study on the growth process of interfacial microbubbles in an air-supersaturated solution, Colloids Surf. A Physicochem. Eng. Asp. 673 (2023) 131879, https://doi.org/10.1016/j.colsurfa.2023.131879.
[15] K.T. Kubra, M.S. Salman, M.N. Hasan, Enhanced toxic dye removal from wastewater using biodegradable polymeric natural adsorbent, J. Mol. Liq. 328 (2021) 115468, https://doi.org/10.1016/j.molliq.2021.115468.
[16] A. Shahat, K.T. Kubra, M.S. Salman, M.N. Hasan, M.M. Hasan, Novel solid-state sensor material for efficient cadmium(II) detection and capturing from wastewater, Microchem. J. 164 (2021) 105967, https://doi.org/10.1016/j.microc.2021.105967.
[17] A.I. Rasee, E. Awual, A.I. Rehan, M.S. Hossain, R.M. Waliullah, K.T. Kubra, M. C. Sheikh, M.S. Salman, M.N. Hasan, M.M. Hasan, et al., Efficient separation, adsorption, and recovery of Samarium(III) ions using novel ligand-based composite adsorbent, Surf. Interfaces 41 (2023) 103276, https://doi.org/10.1016/j.surfin.2023.103276.
[18] M.S. Salman, M.N. Hasan, K.T. Kubra, M.M. Hasan, Optical detection and recovery of Yb(III) from waste sample using novel sensor ensemble nanomaterials, Microchem. J. 162 (2021) 105868, https://doi.org/10.1016/j.microc.2020.105868.
[19] K.T. Kubra, M.M. Hasan, M.N. Hasan, M.S. Salman, M.A. Khaleque, M.C. Sheikh, A. I. Rehan, A.I. Rasee, R.M. Waliullah, M.E. Awual, et al., The heavy lanthanide of Thulium(III) separation and recovery using specific ligand-based facial composite adsorbent, Colloids Surf. A Physicochem. Eng. Asp. 667 (2023) 131415, https://doi.org/10.1016/j.colsurfa.2023.131415.
[20] M.M. Hasan, K.T. Kubra, M.N. Hasan, M.E. Awual, M.S. Salman, M.C. Sheikh, A. I. Rehan, A.I. Rasee, R.M. Waliullah, M.S. Islam, et al., Sustainable ligand-modified based composite material for the selective and effective cadmium(II) capturing from wastewater, J. Mol. Liq. 371 (2023) 121125, https://doi.org/10.1016/j.molliq.2022.121125.
[21] M.N. Hasan, M.S. Salman, M.M. Hasan, K.T. Kubra, M.C. Sheikh, A.I. Rehan, A. I. Rasee, M.E. Awual, R.M. Waliullah, M.S. Hossain, et al., Assessing sustainable Lutetium(III) ions adsorption and recovery using novel composite hybrid nanomaterials, J. Mol. Struct. 1276 (2023) 134795, https://doi.org/10.1016/j.molstruc.2022.134795.
[22] W. Raza, K. Ahmad, F. Alharethy, H. Kim, Designing of Ag decorated ZnO catalyst for on-demand and sustainable H2 production at room temperature, Colloids Surf. A Physicochem. Eng. Asp. 673 (2023) 131757, https://doi.org/10.1016/j.colsurfa.2023.131757.
[23] A.L. Gusev, A.M. Gafarov, P.H. Suleymanov, I.A. Habibov, R.K. Malikov, Y. H. Hasanov, A.I. Levina, P. Mikheev, R.A. Ufa, Some aspects of reliability prediction of chemical industry and hydrogen energy facilities (vessels, machinery and equipment) operated in emergency situations and extreme conditions, Int. J. Hydrog. Energy 86 (2024) 482–510, https://doi.org/10.1016/j.ijhydene.2024.07.462.
[24] M.C. Sheikh, M.M. Hasan, M.N. Hasan, M.S. Salman, K.T. Kubra, M.E. Awual, R. M. Waliullah, A.I. Rasee, A.I. Rehan, M.S. Hossain, et al., Toxic cadmium(II) monitoring and removal from aqueous solution using ligand-based facial composite adsorbent, J. Mol. Liq. 389 (2023) 122854, https://doi.org/10.1016/j.molliq.2023.122854.
[25] A. Islam, S.H. Teo, M.T. Islam, A.H. Mondal, H. Mahmud, S. Ahmed, M. Ibrahim, Y. H. Taufiq-Yap, A.-A. G, M.L. Hossain, et al., Harnessing visible light for sustainable biodiesel production with Ni/Si/MgO photocatalyst, Renew. Sustain. Energy Rev. 208 (2025) 115033, https://doi.org/10.1016/j.rser.2024.115033.
[26] M.R. Awual, M.M. Hasan, H. Znad, Organic–inorganic based nano-conjugate adsorbent for selective palladium(II) detection, separation and recovery, Chem. Eng. J. 259 (2015) 611–619, https://doi.org/10.1016/j.cej.2014.08.028.
[27] M.R. Awual, Novel nanocomposite materials for efficient and selective mercury ions capturing from wastewater, Chem. Eng. J. 307 (2017) 456–465, https://doi.org/10.1016/j.cej.2016.08.108.
[28] J. Defaye, J.M. García Fernández, C. Ortiz Mellet, Les cyclodextrines en pharmacie: perspectives pour le ciblage d'actifs thérapeutiques et le contrôle d'interactions membranaires, Ann. Pharm. Françaises 65 (1) (2007) 33–49, https://doi.org/10.1016/S0003-4509(07)90015-2.
[29] M. Tannous, F. Caldera, G. Hoti, U. Dianzani, R. Cavalli, F. Trotta, Drug-encapsulated cyclodextrin nanosponges, Methods Mol. Biol. 2207 (2021) 247–283, https://doi.org/10.1007/978-1-0716-0920-0_19.
[30] M.A. Esteso, C.M. Romero, Cyclodextrins: properties and applications, Int. J. Mol. Sci. 25 (8) (2024) 4547, https://doi.org/10.3390/ijms25084547.
[31] A. Khurshid, Z. Anwar, A. Khurshid, S. Ahmed, M.A. Sheraz, I. Ahmad, Chapter five - cyclodextrins and their applications in pharmaceutical and related fields, Profiles Drug Subst. Excip. Relat. Methodol. 50 (2025) 183–227, https://doi.org/10.1016/bs.podrm.2024.09.003.
[32] H. Brittain, Profiles of drug substances, excipients, and related methodology, Anal. Profiles Drug Subst. Excip. 29 (2002) 1–5, https://doi.org/10.1016/S1075-6280(02)29002-3.
[33] Khushbu, R. Jindal, Cyclodextrin mediated controlled release of edaravone from pH-responsive sodium alginate and chitosan based nanocomposites, Int. J. Biol. Macromol. 202 (2022) 11–25, https://doi.org/10.1016/j.ijbiomac.2022.01.001.
[34] L.A. Omtvedt, K.A. Kristiansen, W.I. Strand, F.L. Aachmann, B.L. Strand, D. S. Zaytseva-Zotova, Alginate hydrogels functionalized with β-cyclodextrin as a local paclitaxel delivery system, J. Biomed. Mater. Res. 109 (12) (2021) 2625–2639, https://doi.org/10.1002/jbm.a.37255.
[35] L.A. Omtvedt, M.Ø. Dalheim, T.T. Nielsen, K.L. Larsen, B.L. Strand, F.L. Aachmann, Efficient grafting of cyclodextrin to alginate and performance of the hydrogel for release of model drug, Sci. Rep. 9 (1) (2019) 9325, https://doi.org/10.1038/s41598-019-45761-4.
[36] E.-M. Saitani, N. Pippa, D.R. Perinelli, A. Forys, P. Papakyriakopoulou, N. Lagopati, G. Bonacucina, B. Trzebicka, M. Gazouli, S. Pispas, et al., PEO-b-PCL/Tween 80/cyclodextrin systems: from bioinspired fabrication to possible nasal administration of ropinirole hydrochloride, J. Mater. Chem. B 12 (27) (2024) 6587–6604, https://doi.org/10.1039/D4TB00489B.
[37] E.-M. Saitani, N. Pippa, D.R. Perinelli, A. Forys, P. Papakyriakopoulou, N. Lagopati, G. Bonacucina, B. Trzebicka, M. Gazouli, S. Pispas, et al., Fabricating polymer/surfactant/cyclodextrin hybrid particles for possible nose-to-brain delivery of ropinirole hydrochloride: in vitro and ex vivo evaluation, Int. J. Mol. Sci. 25 (2) (2024) 1162, https://doi.org/10.3390/ijms25021162.
[38] S.-R. Ignat, S. Dinescu, J. Váradi, F. Fenyvesi, T.L.P. Nguyen, A. Ciceu, A. Hermenean, M. Costache, Complexation with random methyl-β-cyclodextrin and (2-Hydroxypropyl)-β-cyclodextrin promotes chrysin effect and potential for liver fibrosis therapy, Materials 13 (21) (2020) 5003, https://doi.org/10.3390/ma13215003.
[39] E. Morales, M. Quilaqueo, R. Morales-Medina, S. Drusch, R. Navia, A. Montillet, M. Rubilar, D. Poncelet, F. Galvez-Jiron, F. Acevedo, Pectin–chitosan hydrogel beads for delivery of functional food ingredients, Foods 13 (18) (2024) 2885, https://doi.org/10.3390/foods13182885.
[40] G. Pasparakis, N. Bouropoulos, Swelling studies and in vitro release of verapamil from calcium alginate and calcium alginate–chitosan beads, Int. J. Pharm. 323 (1) (2006) 34–42, https://doi.org/10.1016/j.ijpharm.2006.05.054.
[41] S. Takka, A. Gürel, Evaluation of chitosan/alginate beads using experimental design: formulation and in vitro characterization, AAPS PharmSciTech 11 (1) (2010) 460–466, https://doi.org/10.1208/s12249-010-9406-z.
[42] I. Colinet, V. Dulong, G. Mocanu, L. Picton, D. Le Cerf, New amphiphilic and pH-sensitive hydrogel for controlled release of a model poorly water-soluble drug, Eur. J. Pharm. Biopharm. 73 (3) (2009) 345–350, https://doi.org/10.1016/j.ejpb.2009.07.008.
[43] R.M. Waliullah, A.I. Rehan, M.E. Awual, A.I. Rasee, M.C. Sheikh, M.S. Salman, M. S. Hossain, M.M. Hasan, K.T. Kubra, M.N. Hasan, et al., Optimization of toxic dye removal from contaminated water using chitosan-grafted novel nanocomposite adsorbent, J. Mol. Liq. 388 (2023) 122763, https://doi.org/10.1016/j.molliq.2023.122763.
[44] M.S. Salman, M.N. Hasan, M.M. Hasan, K.T. Kubra, M.C. Sheikh, A.I. Rehan, R. M. Waliullah, A.I. Rasee, M.E. Awual, M.S. Hossain, et al., Improving copper(II) ion detection and adsorption from wastewater by the ligand-functionalized composite adsorbent, J. Mol. Struct. 1282 (2023) 135259, https://doi.org/10.1016/j.molstruc.2023.135259.
[45] H. Md. Munjur, M.N. Hasan, M.R. Awual, M.M. Islam, M.A. Shenashen, J. Iqbal, Biodegradable natural carbohydrate polymeric sustainable adsorbents for efficient toxic dye removal from wastewater, J. Mol. Liq. 319 (2020) 114356, https://doi.org/10.1016/j.molliq.2020.114356.
[46] M.R. Awual, M.M. Hasan, A. Islam, M.M. Rahman, A.M. Asiri, M.A. Khaleque, M. C. Sheikh, Introducing an amine functionalized novel conjugate material for toxic nitrite detection and adsorption from wastewater, J. Clean. Prod. 228 (2019) 778–785, https://doi.org/10.1016/j.jclepro.2019.04.280.
[47] C.-H. Nguyen, K.-S. Banh, C.-H. Dang, C.-H. Nguyen, T.-D. Nguyen, β-cyclodextrin/alginate nanoparticles encapsulated 5-fluorouracil as an effective and safe anticancer drug delivery system, Arab. J. Chem. 15 (6) (2022) 103814, https://doi.org/10.1016/j.arabjc.2022.103814.
[48] N. Kučuk, M. Primožič, Ž. Knez, M. Leitgeb, Alginate beads with encapsulated bioactive substances from Mangifera indica peels as promising peroral delivery systems, Foods 13 (15) (2024) 2404, https://doi.org/10.3390/foods13152404.
[49] B. Mandal, K.S. Alexander, A.T. Riga, Evaluation of the drug-polymer interaction in calcium alginate beads containing diflunisal, Die Pharmazie 65 (2) (2010) 106–109.
[50] A.A.H. Abdellatif, M.A. Ibrahim, M.A. Amin, H. Maswadeh, M.N. Alwehaibi, S. N. Al-Harbi, Z.A. Alharbi, H.A. Mohammed, A.B.M. Mehany, I. Saleem, Cetuximab conjugated with octreotide and entrapped calcium alginate-beads for targeting Somatostatin receptors, Sci. Rep. 10 (1) (2020) 4736, https://doi.org/10.1038/s41598-020-61605-y.
[51] E.-M. Saitani, D. Selianitis, N. Pippa, S. Pispas, G. Valsami, Cyclodextrins-block copolymer drug delivery systems: from design and development to preclinical studies, Nanotechnol. Rev. 13 (1) (2024), https://doi.org/10.1515/ntrev-2023-0204.
[52] M.R. Awual, M.N. Hasan, M.M. Hasan, M.S. Salman, M.C. Sheikh, K.T. Kubra, M. S. Islam, H.M. Marwani, A. Islam, M.A. Khaleque, et al., Green and robust adsorption and recovery of Europium(III) with a mechanism using hybrid donor conjugate materials, Sep. Purif. Technol. 319 (2023) 124088, https://doi.org/10.1016/j.seppur.2023.124088.
[53] M.M. Hasan, M.A. Shenashen, M.N. Hasan, H. Znad, M.S. Salman, M.R. Awual, Natural biodegradable polymeric bioadsorbents for efficient cationic dye encapsulation from wastewater, J. Mol. Liq. 323 (2021) 114587, https://doi.org/10.1016/j.molliq.2020.114587.
[54] M.S. Salman, M.C. Sheikh, M.M. Hasan, M.N. Hasan, K.T. Kubra, A.I. Rehan, M. E. Awual, A.I. Rasee, R.M. Waliullah, M.S. Hossain, et al., Chitosan-coated cotton fiber composite for efficient toxic dye encapsulation from aqueous media, Appl. Surf. Sci. 622 (2023) 157008, https://doi.org/10.1016/j.apsusc.2023.157008.

[55] M.R. Awual, N.H. Alharthi, Y. Okamoto, M.R. Karim, M.E. Halim, M.M. Hasan, M. M. Rahman, M.M. Islam, M.A. Khaleque, M.C. Sheikh, Ligand field effect for Dysprosium(III) and Lutetium(III) adsorption and EXAFS coordination with novel composite nanomaterials, Chem. Eng. J. 320 (2017) 427–435, https://doi.org/10.1016/j.cej.2017.03.075.

[56] M.R. Awual, M.M. Hasan, M.M. Rahman, A.M. Asiri, Novel composite material for selective copper(II) detection and removal from aqueous media, J. Mol. Liq. 283 (2019) 772–780, https://doi.org/10.1016/j.molliq.2019.03.141.

[57] C. Zohar-Perez, I. Chet, A. Nussinovitch, Irregular textural features of dried alginate–filler beads, Food Hydrocoll. 18 (2) (2004) 249–258, https://doi.org/10.1016/S0268-005X(03)00081-X.

[58] K. Haldar, S. Chakraborty, Investigation of chemical reaction during sodium alginate drop impact on calcium chloride film, Phys. Fluids 31 (7) (2019), https://doi.org/10.1063/1.5100243.

[59] S.L. Fegade, Green hydrocarbons and fuels from municipal polymer waste co-fed with natural gas using a batch catalytic slurry process, Green Technol. Sustain. 2 (3) (2024) 100099, https://doi.org/10.1016/j.grets.2024.100099.